Follow the water: Connecting a CO_2 reservoir and bleached sandstone to iron-rich concretions in the Navajo Sandstone of south-central Utah, USA

David B. Loope[1], Richard M. Kettler[1], and Karrie A. Weber[1,2]
[1]Department of Earth and Atmospheric Sciences, University of Nebraska, Lincoln, Nebraska 68588-0340, USA
[2]School of Biological Sciences, University of Nebraska, Lincoln, Nebraska 68588-0118, USA

ABSTRACT

Concretions with thick, iron oxide–cemented rinds and lightly cemented, iron-poor sandstone cores are abundant within the Navajo Sandstone near the southeast flank of the Escalante anticline (Utah, United States). Previous workers suggested the spheroidal concretions as analogs for Martian "blueberries" (hematite concretions), and linked the origin of concretions and bleaching of the Navajo Sandstone to the buoyant rise of hydrocarbons toward anticlinal crests. We measured azimuths of 163 pipe-like (pipy), joint-associated concretions and those of 58 "comet tails" that extend from some spherical concretions. Both data sets have vector magnitudes >90%, and subparallel, southeast-directed resultant vectors. Our data indicate that groundwater transported and deposited iron over a flow path that spanned more than 100 km from the anticlinal crest to the Colorado River. Buoyant fluids could not have transported iron from bleached rock to sites of concretion growth, however, because iron moved downdip. We propose that iron was transported southeastward by reducing groundwater that flowed through a CO_2- and methane-charged reservoir within the Escalante anticline. Iron-rich carbonates precipitated during CO_2 degassing. After methane was flushed from the aquifer, microaerophiles oxidized Fe^{2+} in concretions, dissolving the carbonates and forming the iron oxide–rich rinds and iron-poor cores. These concretions define the flow direction and geochemical evolution of a paleoaquifer. This approach could be used to follow the water on other planets.

INTRODUCTION

The Jurassic Navajo Sandstone is spectacularly exposed in canyons that are being cut through the cores and flanks of Laramide anticlines during the continuing uplift of the Colorado Plateau (western United States). Spheroidal, iron oxide–rich concretions (Fig. 1) are common within this unit in southern Utah and have been suggested as Earth analogs for the Martian "blueberries" (hematite concretions) imaged by the rover *Opportunity* (Chan et al., 2004). Although eolian grains in the Navajo Sandstone were probably reddened during an earlier stage of diagenesis, much of the rock exposed on the flanks and cores of five Colorado Plateau anticlines is now bleached (Beitler et al., 2003). Iron mobilized during bleaching events has been proposed as the likely source for the iron in the concretions. According to Beitler et al. (2003, 2005), buoyant, updipmigrating hydrocarbons bleached the sandstone and transported the iron to sites where concretions formed. Here we demonstrate that the fluid that cemented the concretions moved downdip, away from the bleached sandstone on the structural high. Buoyant fluids could not have transported the bulk of the iron. Our model uses groundwater to bleach the sandstones and move the iron to sites of concretion growth. If the Navajo Sandstone concretions are analogous to the Martian concretions, indicators of flow direction analogous to those described here
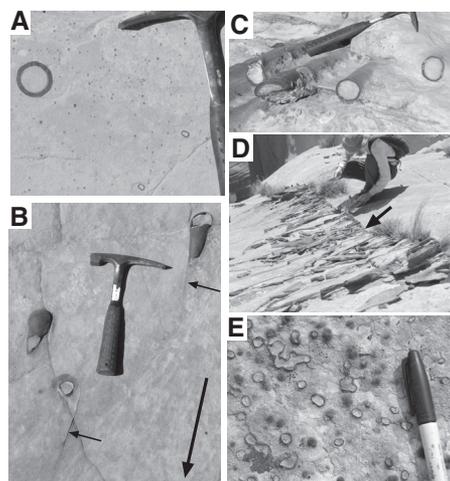
Figure 1. In situ iron oxide–rich spheroids and pipes. A: Spheroids with iron oxide–cemented rinds around iron-poor cores. Hammer is 28 cm long. B: Spheroid and two ovoid concretions with iron oxide comet tails (small arrows) extending southeastward (large arrow). Note that long axes of ovoids are parallel to comet tails. C: Six iron oxide–cemented pipes; four show iron-rich rinds around iron-poor cores. Pipes are parallel, oriented northwest-southeast, and extend southeast from vertical joint ~1 m beyond upper right corner. D: Iron oxide pipes extending southeast (toward lower left) from near-vertical joint (arrow). E: Complex iron oxide–cemented rinds. Irregular shapes resulted from microbial oxidation of clustered, intergrown siderite concretions. (Pen cap is 5 cm long.)

could be identified and mapped using remotely controlled vehicles. The data obtained would provide insights into the history of subsurface fluids and water-rock interaction. Here we also argue that (1) methane dissolved in groundwater (much more widespread in the solar system than buoyant fluids composing longer chain hydrocarbons) reduced and mobilized the iron; (2) iron-rich carbonates were the original cements within the concretions; and (3) microbial oxidative dissolution of iron-rich carbonates led to the formation iron oxide–rich concretions. These concretions provide the necessary clues for investigators to follow the water (e.g., Hubbard et al., 2002) and build testable models of flow systems on Earth and other planets.

GEOLOGIC SETTING

Hydrodynamic History

The Escalante and Upper Valley anticlines are north-trending, Laramide structures located south of the Aquarius Plateau in south-central Utah (Fig. 2). These structures plunge to the southeast, where the Navajo is conformably overlain by the evaporites and mudstone of the Jurassic Carmel Formation; to the north the structures are capped by Tertiary andesites on the Aquarius Plateau (Fig. 2). The Escalante River drains the high elevations of the Aquarius Plateau, dissects the southern end of the Escalante anticline, and flows southeastward to join the Colorado River in Glen Canyon (Fig. 2). Exposure of the Navajo Sandstone in the anticline is a recent event, a product of uplift of the Colorado Plateau within the past 6 m.y. (Karlstrom et al., 2008).

The Paleozoic and Mesozoic sedimentary rocks of the study area compose highly permeable aquifers and reservoirs separated by sealing lithologies. At the Upper Valley Field, 15 km west of Escalante, Utah (Fig. 2), the Triassic Moenkopi Formation seals petroleum and natural gas trapped within the Permian Kaibab Formation and Timpoweap Member of the Moenkopi Formation (Allin, 1993). Tar sands are present in the Moenkopi and Chinle Formations on the Circle Cliffs uplift (Allison, 1997). Carbon dioxide accumulations are widespread on the Colorado Plateau; at least 11 anticlines contain trapped CO_2 (Shipton et al., 2005;
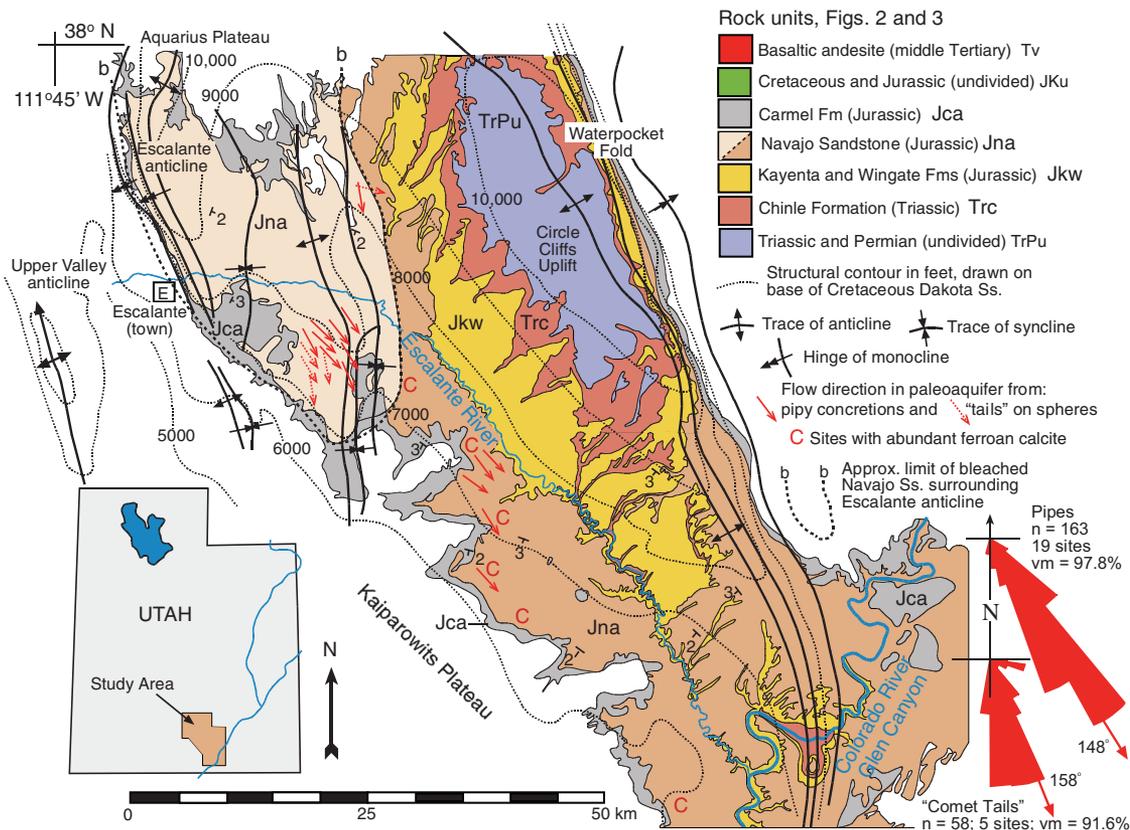
Figure 2. Geologic map of study area with rose diagrams, resultant vectors, and vector magnitudes (vm; Potter and Pettijohn, 1977) for pipes and "comet tails." Area of bleached sandstone is from Beitler et al. (2003).

Haszeldine et al., 2005), and much of this gas is of mantle origin (Crossey et al., 2006; 2009; Gilfillan et al., 2008). The Escalante anticline holds an estimated 1.5–4 trillion cubic feet of gas (93%–99% CO_2, 1%–6% N_2, 0.4%–0.7% CH_4; Allison, 1997) within a 600-m-thick reservoir, largely of Permian age. Whereas petroleum shows, staining, and production are confined to Triassic and older rocks (Allison, 1997), CO_2 leaks through the Triassic sealing lithologies along faults (Shipton et al., 2005).

Uplift and dissection of the Colorado Plateau changed the hydrodynamics of the study area. Fluids that migrated into anticlines under an earlier, buoyancy-dominated regime were flushed to the Colorado River when groundwater circulated vigorously through the former reservoir rocks. A strong southeastward hydrodynamic drive (broadly parallel to the direction of surface water drainage in the region) has driven oil beyond the crest of the structure in the Upper Valley Field, leaving a tilted oil-water contact (Allin, 1990).

Bleaching and Concretions

The Navajo Sandstone is white within the Escalante anticline, but is stained red to the southeast, where gently dipping homoclinal beds are exposed along the Escalante River (Fig. 2). Beitler et al. (2003) related this color contrast to bleaching by buoyant, reducing fluids that migrated through the Navajo Sandstone and accumulated in the anticlinal crests to produce giant hydrocarbon reservoirs.

Southeast of the Escalante anticline, outcrops of light colored Navajo Sandstone contain abundant 0.5-mm-diameter to 20-cm-diameter, spheroidal concretions composed of 0.1–10-mm-thick rinds of iron oxide–cemented sandstone surrounding iron-poor, friable sandstone cores (Fig. 1A). Iron oxide stains resembling comet tails extend 10–20 cm southeastward away from individual spheroids and rare ovoids (Fig. 1B; Chan et al., 2000; Busigny and Dauphas, 2007). Spheroidal concretions are most abundant near the transition from bleached rocks (updip) to unbleached red rocks (downdip) (Fig. 2).

Pipe-like (pipy) concretions, also with iron oxide–cemented rims and friable sandstone cores, are 3–30 cm in diameter and can be as long as 4 m. These concretions occur as groups of near horizontal, subparallel pipes that extend southeastward into wall rock from northeast-trending joints (Figs. 1C and 1D). Large pipes (diameter, d >10 cm) are abundant in bleached sandstone just west of the boundary with

unbleached rock (Fig. 2), but pipes become smaller and much less common southeastward from that boundary.

Within locally bleached beds, spheroidal concretions cemented by ferroan calcite are abundant southeast of the pervasively bleached Navajo Sandstone (Fig. 2; Fig. DR1 in the GSA Data Repository[1]). Isolated concretionary masses (5 m < d < 10 m) of sandstone cemented by poikilotopic ferroan calcite are distributed through the upper 100 m of the formation. This ferroan-calcite zone overlaps the southeast end of the zone with pipy iron oxide concretions (Fig. 2). Where calcite is abundant, however, iron oxide–rich concretions are small and rare. Where iron oxide–rich concretions are abundant, calcite is rare (Fig. 2; Beitler et al., 2005).

RESULTS AND DISCUSSION

Evidence for Southeastward Transport of Iron

We measured the orientations of the comet tails of 58 spheroids at 5 sites, and of 163 pipy concretions at 19 sites For both features, the azimuth was considered to be the direction of extension away from the adjacent spheroid or joint (Fig. 1). The measured vector means of comet tails (158°) and pipy concretions (148°)

are subparallel; both data sets have vector magnitudes >90% (Fig. 2; Fig. DR1).

Mapped vectors parallel the flow direction of the modern Escalante River (Fig. 2). Aquifers that have been dissected and drained recently should show evidence of the same flow direction as modern surface water. The pipy concretions in the Navajo Sandstone parallel surface water flow in the same way that elongate concretions elsewhere have been shown to parallel the regional paleoslope (e.g., Schultz, 1941; Johnson, 1989; Cavazza et al., 2009).

We interpret pipy concretions and comet tails as products of iron-bearing groundwater that flowed southeastward through jointed rock. The orientations of comet tails were first measured by Chan et al. (2000), who examined Navajo Sandstone concretions in eastern Utah, but considered the groundwater flow system that formed the comet tails to be distinct from the one that transported the iron during concretion growth. We observed comet tails oriented parallel not only to pipy concretions, but also to the direction of elongation of ovoid concretions among the more common spheroids (Fig. 1B). Iron in both the concretions and comet tails was transported by the same flow system.

The new directional data indicate that groundwater moved iron downdip from bleached rock on the crest and flanks of the Escalante anticline, but many questions remain. How was groundwater able to transport iron? Why do pipy concretions extend from the southeast sides of joints? Why are ferran calcite concretions southeast of iron oxide–rich, non-calcitic concretions? Why does iron oxide cement in the non-calcitic concretions form dense rinds around iron-poor sandstone cores? Is the iron oxide cement is a primary or secondary precipitate? The remainder of this paper addresses these issues.

Flushing the Escalante Anticline

Leaching of iron from the Navajo Sandstone and transport in aqueous solution requires reducing waters. We hypothesize that meteoric water falling on the Aquarius Plateau recharged the Navajo Sandstone aquifer (Fig. 3). This groundwater became charged with CH_4 and CO_2 as it flowed through and displaced gas in the Escalante anticline (Fig. 3; Fig. DR1). Reducing waters bleached the sandstone and transported sufficient ferrous iron to form the concretions. We favor CH_4- and CO_2-charged groundwater as an iron transport medium for three reasons. (1) There is no bitumen in the Navajo Sandstone in the area. (2) Early Triassic and older strata in the Escalante anticline host CO_2 and CH_4. (3) Grain-coating iron oxides are unstable when they are in contact with waters that have equilibrated with a gas phase similar to that found in the Escalante anticline today (Fig. DR1).

Joints and Degassing

Before exhumation, the Navajo aquifer was confined by the Carmel Formation (Fig. 3). The piezometric head for any point in an aquifer is the sum of the elevation head and the pressure head (e.g., Hubbert, 1953). Upon incision of the Carmel seal by the Colorado River, the pressure head at the distal end of the Navajo aquifer was reduced to atmospheric pressure. The hydraulic gradient thus increased and the pressure head on the eastern limb of the anticline decreased (Fig. 3; Fig. DR1). The decline in pressure head resulted in exsolution of a CO_2-rich gas phase; the aquifer degassed along joints.

Carbonate Precursors

Curtis and Coleman (1986, p. 23) noted that carbonate minerals are the most common concretionary cements, and that "…iron oxides and hydrated iron oxides are most probably secondary oxidation products when seen in ancient concretions." We propose that all iron oxide–rich concretions in the Navajo Sandstone were originally cemented by iron-rich carbonate minerals; the iron oxide cements are not primary precipitates (cf. Chan et al., 2004, 2005; Beitler et al., 2005).

The occurrence of ferran calcite concretions downdip from the iron oxide–rich concretions is evidence that the aquifer was filled with iron and CO_2-charged water (Figs. 2 and 3). The rise in pH as the aquifer degassed along joints

Figure 3. A: Northwest-southeast schematic cross section showing progressive dissection of study area during uplift of Colorado Plateau. Arrows follow water within confined Navajo aquifer that, ca. 1 Ma, flowed through CO_2- and CH_4-charged Escalante anticline; reduced water (blue arrows) precipitated iron-rich carbonate concretions (dark blue—siderite; light blue—ferran calcite), and discharged on walls of ancestral Colorado River canyon. See Figure 2 for rock units and geography, and Figure DR1 (see footnote 1) for animations of fluid flow and concretion growth and/or dissolution. B: Sequence and approximate timing of structural, erosional, and diagenetic events. Iron-rich concretions were oxidized only after CH_4 had been flushed from anticline.

caused carbonate minerals (ferroan calcite and probably siderite) to precipitate immediately down gradient of the joints. Mass-balance considerations support the hypothesis that siderite was the precursor to the iron oxide concretion. A typical rinded concretion (Fig. 1A) comprises 17% Fe_2O_3, has a bulk density of 4 g mL^{-1}, and has an interior with 27% porosity. Solid siderite concretions would contain the same amount of iron as rinded concretions of the same diameter. However, a concretion cemented by calcite with 10 mol% Fe would hold only 8% of the iron contained in a rinded concretion of the same diameter (Fig. DR1). Siderite precipitation in the upper reaches of the aquifer would have depleted iron dissolved in the groundwater, leading to down-gradient precipitation of ferroan calcite as degassing of the water continued at lower elevations.

The Colorado River began cutting the Navajo Sandstone near the mouth of the Escalante River ~2 m.y. ago (Karlstrom et al., 2008; Cook et al., 2009); therefore, the carbonate concretions began to form during the early Pleistocene.

Formation of Iron Oxide Rinds

Although oxidation of ferrous carbonate minerals in oxygenated pore water may occur abiotically, microbial metabolism is an alternative mechanism. Iron redox reactions are commonly linked to microbial respiration where Fe(II) serves as an electron donor and molecular oxygen, nitrate, or perchlorate serve as terminal electron acceptors (e.g., Weber et al., 2006; Ehrlich and Newman, 2009). We hypothesize that, with continued recharge, the reduced waters from which the ferrous carbonates had precipitated were flushed by oxidizing waters (Fig. 3; Fig. DR1). Microaerophilic, iron-oxidizing microorganisms then colonized the surfaces of concretions that were pervasively cemented by siderite. Metabolic activity of these organisms (Emerson and Moyer, 1997; Druschel et al., 2008) maintained a reducing microenvironment just beneath the concretion surface. Iron oxidation at the oxic-anoxic interface generated acid:

$$4Fe_{(aq)}^{2+} + O_{2(aq)} + 10H_2O$$

$$= 4Fe(OH)_{3(am)} + 8H_{(aq)}^+ \qquad (1)$$

that dissolved the siderite cement (aq—aqueous; am—amorphous).

$$FeCO_{3(siderite)} + H_{(aq)}^+ = Fe_{(aq)}^{2+} + HCO_{(aq)}^-. \quad (2)$$

The net reaction produced excess acid and was therefore self-promoting:

$$4FeCO_{3(siderite)} + O_{2(aq)} + 10H_2O$$

$$= 4Fe(OH)_{3(am)} + 4HCO_{(aq)}^- + 4H_{(aq)}^+. \quad (3)$$

The liberated ferrous iron diffused from the interior to the perimeter of the concretions where it was oxidized to form the rind. Ferron calcite, however, yields much less iron and consumes acid under oxidizing conditions:

$$64Fe_{0.0625}Ca_{0.9375}CO_{3(siderite)} + O_{2(aq)} + 10H_2O + 56H^+_{(aq)}$$

$$= 4Fe(OH)_{3(am)} + 64HCO^-_{3(aq)} + 60Ca^{2+}_{(aq)}. \quad (4)$$

Whereas siderite dissolves during oxidation, leaving iron oxide as a product; oxidation of ferroan calcite requires either copious acid (from another source) or precipitation of calcium carbonate. Calcite-cemented concretions are absent from the upper reaches of the system because oxidation of siderite generated sufficient acid to dissolve them. Because our hypothesis for the origin of the rinds calls on migration of iron from the cores of thoroughly cemented concretions, it can better explain the amalgamated rinds generated during dissolution of intergrown concretions (Fig. 1E).

The amount of groundwater and oxygen required to effect the oxidation is not excessive. A 170 g concretion cemented with 34 g of siderite (25% porosity) can be oxidized during the passage of groundwater contained in an ~6.3-km-long cylinder of saturated Navajo Sandstone that has the same porosity and cross-sectional area as the concretion (assuming that the O_2 concentration of groundwater is 30 µmol kg^{-1}).

Using scanning electron microscopy on iron oxide–encrusted sand grains along the inner surface of the rinds, we have imaged abundant iron-coated tubules that are several microns long and <1 µm in diameter (Spanbauer et al., 2009). We interpret these tubules as the fossilized remains of iron-oxidizing microbes.

CONCLUSIONS

Our new model for the formation of the Navajo concretions comprises six elements. (1) Iron was transported downdip from bleached zones by reducing, aqueous fluids. (2) The groundwater flow system that transported the iron flowed southeastward, parallel to the modern drainage. (3) Methane and CO_2 in the ancient groundwater allowed it to carry copious reduced iron down gradient. (4) Incision of the Navajo Sandstone in Glen Canyon caused an increase in the hydraulic gradient and decrease in the pressure head of the Navajo Sandstone aquifer. (5) Degassing of CO_2 from the groundwater raised its pH, leading to precipitation of carbonate concretions. (6) The primary concretions were colonized by iron-oxidizing microbes that generated the iron oxide–rich rinds that now surround iron-poor cores.

REFERENCES CITED

Allin, D.L., 1990, Colorado Plateau sub-surface water flow key: Oil & Gas Journal, v. 88, no. 30, p. 52–54.

Allin, D.L., 1993, Upper Valley, in Hill, B.G., and Bereskin, S.R., eds., Oil and gas fields of Utah: Utah Geological Association Publication 22, 192 p.

Allison, M.L., compiler, 1997, A preliminary assessment of energy and mineral resources within the Grand Staircase–Escalante National Monument: Utah Geological Survey Circular, v. 93, 35 p., http://geology.utah.gov/online/c/c-93/index.htm.

Beitler, B., Chan, M.A., and Parry, W.T., 2003, Bleaching of Jurassic Navajo Sandstone on Colorado Plateau Laramide highs: Evidence of exhumed hydrocarbon supergiants?: Geology, v. 31, p. 1041–1044, doi: 10.1130/G19794.1.

Beitler, B., Parry, W.T., and Chan, M.A., 2005, Fingerprints of fluid flow: Chemical diagenetic history of the Jurassic Navajo Sandstone, southern Utah, U.S.A: Journal of Sedimentary Research, v. 75, p. 547–561, doi: 10.2110/jsr.2005.045.

Busigny, V., and Dauphas, N., 2007, Tracing paleofluid circulations using iron isotopes: A study of hematite and goethite concretions from the Navajo Sandstone (Utah, USA): Earth and Planetary Science Letters, v. 254, p. 272–287, doi: 10.1016/j.epsl.2006.11.038.

Cavazza, W., Braga, R., Reinhardt, E.G., and Zanotti, C., 2009, Influence of host-rock texture on the morphology of carbonate concretions in a meteoric diagenetic environment: Journal of Sedimentary Research, v. 79, p. 377–388, doi: 10.2110/jsr.2009.047.

Chan, M.A., Parry, W.T., and Bowman, J.R., 2000, Diagenetic hematite and manganese oxides and fault-related fluid flow in Jurassic sandstones, southeastern Utah: American Association of Petroleum Geologists Bulletin, v. 84, p. 1281–1310.

Chan, M.A., Beitler, B., Parry, W.T., Ormo, J., and Komatsu, G., 2004, A possible terrestrial analogue for haematite concretions on Mars: Nature, v. 429, p. 731–734, doi: 10.1038/nature02600.

Chan, M.A., Bowen, B.B., and Parry, W.T., 2005, Red rock and red planet diagenesis: Comparisons of Earth and Mars concretions: GSA Today, v. 15, no. 8, doi: 10.1130/1052-5173(2005)015<4:RRARPD>2.0.CO;2.

Cook, K.L., Whipple, K.X, Heimsath, A.M., and Hanks, T.C., 2009, Rapid incision of the Colorado River in Glen Canyon—Insights from channel profiles, local incision rates and modeling of lithologic controls: Earth Surface Processes and Landforms, v. 34, p. 994–1010.

Crossey, L.J., Fischer, T.P., Patchett, P.J., Karlstrom, K.E., Hilton, D.R., Newell, D.L., Huntoon, P., and Reynolds, A.C., 2006, Dissected hydrologic system at Grand Canyon: Interaction between upper world and lower world waters in modern springs and travertine: Geology, v. 34, p. 25–28, doi: 10.1130/G22057.1.

Crossey, L.J., Karlstrom, K.E., Springer, A., Newell, D., Hilton, D., and Fischer, T., 2009, Degassing of mantle-derived CO_2 and ^{3}He from springs in the southern Colorado Plateau region—Neotectonic connections and implications for groundwater systems: Geological Society of America Bulletin, v. 121, p. 1034–1053, doi: 10.1130/B26394.1.

Curtis, C.D., and Coleman, M.L., 1986, Controls on the precipitation of early diagenetic calcite, dolomite, and siderite concretions in complex depositional sequences, in Gautier, D.L., ed., Roles of organic matter in sediment diagenesis: Society of Economic Paleontologists and Mineralogists Special Publication 38, p. 23–33.

Druschel, G.K., Emerson, D., Sutka, R., Suchecki, P., Luther, I.I.I., and George, W., 2008, Low-oxygen and chemical kinetic constraints on the geochemical niche of neutrophilic iron(II) oxidizing microorganisms: Geochimica et Cosmochimica Acta, v. 72, p. 3358–3370, doi: 10.1016/j.gca.2008.04.035.

Ehrlich, H.L., and Newman, D.K., 2009, Geomicrobiology (fifth edition): Boca Raton, Florida, CRC Press, 606 p.

Emerson, D., and Moyer, C.L., 1997, Isolation and characterization of novel iron-oxidizing bacteria that grow at circumneutral pH: Applied and Environmental Microbiology, v. 63, p. 4784–4792.

Gilfillan, S.M.V., Ballentine, C.J., Holland, G., Balgburn, D., Sherwood Lollar, B., Stevens, S., Schoell, M., and Cassidy, M., 2008, The noble gas chemistry of natural CO_2 gas reservoirs from the Colorado Plateau and Rocky Mountain Provinces, USA: Geochimica et Cosmochimica Acta, v. 72, p. 1174–1198, doi: 10.1016/j.gca.2007.10.009.

Haszeldine, R.S., Quinn, O., England, G., Wilkinson, M., Shipton, Z.K., Evans, J.P., Heath, J., Crossey, L., Ballentine, C.J., and Graham, C.M., 2005, Natural geochemical analogues for carbon dioxide storage in deep geological porous reservoirs, a United Kingdom perspective: Oil & Gas Science and Technology, v. 60, p. 33–49, doi: 10.2516/ogst:2005004.

Hubbard, G.S., Naderi, F.M., and Garvin, J.B., 2002, Following the water, the new program for Mars exploration: Acta Astronautica, v. 51, p. 337–350, doi: 10.1016/S0094-5765(02)00067-X.

Hubbert, M.K., 1953, Entrapment of petroleum under hydrodynamic conditions: American Association of Petroleum Geologists Bulletin, v. 37, p. 1954–2026.

Johnson, M.R., 1989, Paleogeographic significance of oriented calcareous concretions in the Triassic Katberg Formation, South Africa: Journal of Sedimentary Petrology, v. 59, p. 1008–1010.

Karlstrom, K.E., Crow, R., Crossey, L.J., Coblentz, D., and van Wijk, J., 2008, Model for tectonically driven incision of the less than 6 Ma Grand Canyon: Geology, v. 36, p. 835–838, doi: 10.1130/G25032A.1.

Potter, P.E., and Pettijohn, F.J., 1977, Paleocurrents and basin analysis (second edition): Berlin, Springer-Verlag, 425 p.

Schultz, C.B., 1941, The pipy concretions of the Arikaree: University of Nebraska State Museum Bulletin, v. 2, p. 69–82.

Shipton, Z.K., Evans, J.P., Dockrill, B., Heath, J., Williams, A., Kirchner, D., and Kolesar, P.T., 2005, Natural leaking CO_2-charged systems as analogs for failed geologic storage reservoirs, in Thomas, D.C., and Benson, S.M., eds., Carbon dioxide capture for storage in deep geologic formations, Volume 2: Amsterdam, Elsevier, p. 699–712.

Spanbauer, T.L, Weber, K.A., Kettler, R.M., and Loope, D.B., 2009, Biosignatures in spheroidal iron-oxide-rich concretions from the Navajo Sandstone: American Geophysical Union, Fall Meeting 2009, abs. B23D-0404.

Weber, K.A., Achenbach, L.A., and Coates, J.D., 2006, Microorganisms pumping iron: anaerobic microbial iron oxidation and reduction: Nature Reviews Microbiology, v. 4, p. 752–764, doi: 10.1038/nrmicro1490.